Supplementary Information (SI) for EES Batteries.

Supporting Information

High Al-doping Ration Halide Solid Electrolyte with A 3D Li-ion Transportation Framework

Yi-Xuan Li[a,1], *Li-Ping Cui*[a,1], *Shu Zhang*[a,1], *Peng-Fei Sun*[a], *Cheng-Dong Fang*[a], *Yu-Hang Zhang*[a], *Liu-Bin Feng*[a], *and Jia-Jia Chen*[a,*]

Materials and Methods

1.1 Synthesis of Li_3YCl_6 and $Li_3Al_xY_{1-x}Cl_6$:

All preparations and synthetic procedures were conducted under an argon atmosphere. The solid-state electrolyte (SSE) $Li_3Al_xY_{1-x}Cl_6$ (LAYC) was synthesized from LiCl (Macklin, 99.0%), YCl_3 (Macklin, 99.99%), and $AlCl_3$ (Macklin, 99.99%) in specific ratios. The three components were uniformly mixed in a glove box under argon protection, then transferred to a ball mill (HF-Kejing, MSK-SFM-3-II) and ball-milled at 600 rpm for 20 hours to obtain the ball-milled LAYC sample. The entire ball-milling process was carried out under argon protection, with a ball-to-material ratio of 40:1. The ball-milled LAYC was sealed in a quartz tube under argon and annealed at 550 °C for 4 hours to yield the annealed LAYC at 550 °C. The solid-state electrolyte Li_3YCl_6 was synthesized by ball-milling LiCl and YCl_3 in a 3:1 molar ratio following the same procedure as for LAYC.

1.2 Characterization:

X-ray diffraction (XRD) characterization of LAYC was conducted using a Rigaku Ultima IV with Cu Kα radiation. To avoid the influence of air, the powder sample was sealed with Kapton tape in a glove box under argon protection. X-ray photoelectron spectroscopy (XPS) data were collected on a Thermo Scientific ESCALAB Xi+ using monochromatic Al Kα radiation. Time-of-flight secondary ion mass spectrometry (TOF-SIMS) measurements were performed on an IONTOF M6 at a base pressure of 10^{-9} mbar, using negative ion mode with a detection area of 100×100 μm^2. Samples for XPS and TOF-SIMS were disassembled from Li|LAYC|Li cells after interface reaction completion and were transferred using a vacuum jig to prevent air exposure.

1.3 Electrochemical characterization:

Ion conductivity and activation energy testing: Electrochemical impedance spectroscopy (EIS) measurements were conducted on cold-pressed powder samples using a Solartron 1260. The test frequency ranged from 10 MHz to 1 Hz, with an applied AC bias of 5 mV, over a temperature range from 25 °C to 60 °C. Approximately 200 mg of solid electrolyte powder was cold-pressed into a solid electrolyte disk with a diameter of 16 mm using a mold under a pressure of 5 Tons. Silver was used as the blocking electrode for EIS testing. The entire testing process was carried out under an external pressure of 5 Tons. The activation energy was calculated using a specified formula:

$$\sigma T=\sigma_0 \exp(-E_a / k_B T)$$

where σ is ionic conductivity, σ_0 is the Arrhenius prefactor, T is absolute temperature, E_a is the activation energy, and k_B is the Boltzmann constant.

1.4 Assembly and testing of lithium symmetric cells:

80 mg of solid-state electrolyte powder was compressed into a solid electrolyte disc using a mold with a diameter of 13 mm under a pressure of 2 Tons. Subsequently, metal lithium discs and stainless-steel discs, both with a diameter of 10 mm, were affixed to both sides of the solid electrolyte disc. The Li|SSEs|Li symmetric cells were then assembled using a battery sealer (HF-Kejing, MSK-110) with an applied pressure of 50 kg cm^{-2}.[1] Constant current testing conditions for the lithium symmetric cells were set at 60 °C with a current density of 0.03 mA/cm^2 and at 25 °C with a current density of 0.1 mA/cm^2. The cells were allowed to stabilize for 12 hours before testing to ensure constant temperature. Before the constant current test at 25 °C, the lithium symmetrical battery will be activated at 60 °C for 48 h. Electrochemical impedance spectroscopy (EIS) testing of the lithium symmetric cells was conducted using a Solartron 1260, with a frequency range from 10 MHz to 1 Hz, an applied AC bias of 10 mV, and a testing temperature of 25 °C.

1.5 Cationic polarization factor calculations:

The ionic potential (I) is defined as the ratio of cationic charge (z^+) and cationic radius (r^+), which reflects the polarizing power of cations. The ionic potential gives an indication of the strength of the electrostatic attraction of ions with opposite charges. Aiming at a guide for the crystal structure control of the halide SSEs, we propose the “cationic polarization factor” (τ) to predict the structure of Li_aMX_b halides based on the chemical composition, which hasthe form

$$\tau = \frac{\Sigma\Phi\text{cations}}{\Sigma\Phi\text{X}} = \frac{\Phi\text{Li} + \Sigma\Phi\text{M}}{\Sigma\Phi\text{X}}$$

where ΦLi represents the molar content proportionally ionic potential of lithium ions, which is defined as ΦLi = nLi × ILi; Similarly, ΣΦM and ΣΦX represent the summation of the molar content proportionally ionic potential of different ions[2].

Table S1

Halides	τ	ΦLi	ΦM	ΦX	Structure	Ref
Li_3YCl_6	1.7307	3.3333	2.8846	3.5928	hcp	16
$Li_3Al_{0.1}Y_{0.9}Cl_6$	1.8065	3.3333	3.1569	3.5928	ccp	This work
$Li_3Al_{0.3}Y_{0.7}Cl_6$	1.9580	3.3333	3.7015	3.5928	ccp	This work
$Li_3Al_{0.5}Y_{0.5}Cl_6$	2.1096	3.3333	4.2461	3.5928	ccp	This work
$Li_3Al_{0.7}Y_{0.3}Cl_6$	2.2612	3.3333	4.7906	3.5928	ccp	This work
$Li_3Al_{0.9}Y_{0.7}Cl_6$	2.4127	3.3333	5.3352	3.5928	ccp	This work
$LiAlCl_4$	2.8050	1.1111	5.6075	2.3952	S.G. P21/c	26
Li_3InCl_6	1.8161	3.3333	3.1915	3.5928	ccp	21

1.6 BVSE calculations:

The Bond Valence Site Energy (E_{BVSE}) of A cation can then be interpreted as a result of a Morse-type interaction with the adjacent X anions and the sum of the Coulomb repulsion ($E_{\text{repulsion}}$) of A with other immobile cations[3,4]:

$$E_{\text{BVSE}}(\text{A}) = \sum_{\text{X}} D_0 \left[\sum_{i=1}^{N} \left(\left(\frac{S_{\text{A-X}}}{S_{\text{min,A-X}}} \right)^2 - \frac{2 \cdot S_{\text{A-X}}}{S_{\text{min,A-X}}} \right) \right] + E_{\text{repulsion}}$$

With the help of empirical parameters $R_{0,\text{A-X}}$ and $b_{\text{A-X}}$, an individual bond valence $S_{\text{A-X}}$ is related to the bond length $R_{\text{A-X}}$ between the A cation and an X anion, and the required bond valence parameters R_0 and b can be taken from the soft*BV* database[5]:

$$S_{\mathrm{A-X}} = \exp\left[\frac{R_{0,\mathrm{A-X}} - R_{\mathrm{A-X}}}{b_{\mathrm{A-X}}}\right]$$

Moreover, the Coulomb repulsion is considered only between mobile and immobile cations in order to reveal continuous pathways, while Coulomb attraction terms are generally integrated into the Morse attraction term:

$$E_{\mathrm{repulsion}}(A - B) = \frac{q_{\mathrm{A}} \cdot q_{\mathrm{B}}}{R_{\mathrm{A-B}}} \cdot \mathrm{erfc}\left(\frac{R_{\mathrm{A-B}}}{f \cdot (r_{\mathrm{A}} + r_{\mathrm{B}})}\right)$$

where r_A and r_B are the covalent radii of the respective cation pair (A and B), and f is a screening factor (typically $f \approx 0.75$)[6].

The BVSE analysis was conducted using the softBV program and the energy profiles of the Li ion migration pathways were calculated against a 3D grid of points with 0.1 Å resolution using the transferable Morse-type softBV force field. Firstly, selecting structures of interest and obtaining CIF files ($Li_3Al_{0.3}Y_{0.7}Cl_6$, $Li_3Al_{0.5}Y_{0.5}Cl_6$, $Li_3Al_{0.7}Y_{0.3}Cl_6$). Then, initiating the generation of .cube files-formatted energy landscape files specifying mobile species, screening factor and grid resolution. Finally, running the migration path analyzer on the obtained .cube files to get the migration pathway and migration energy barrier. The enclosed isosurface reflects where Li ions can go through, while the threshold value to form a path is estimated as the Li ions migration energy barrier. During the calculation, the isosurfaces can be displayed by the VESTA visualization package[9].

1. Experimental Data

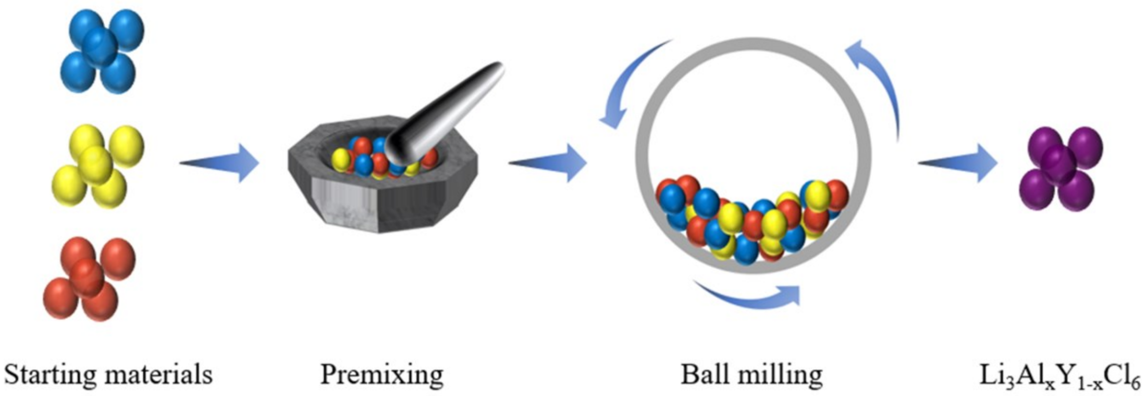

Figure S1. Scheme of the preparation process of $Li^3Al^xY^{1-x}Cl^6$ electrolyte.

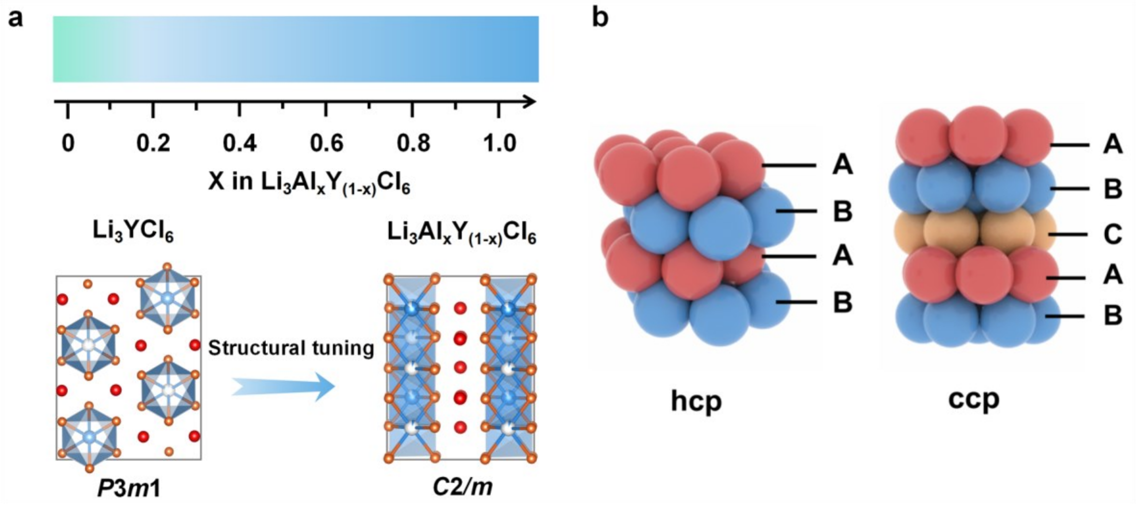

Figure S2. a) Scheme of the structural tuning triggered by the adjustment of the Al^{3+}/Y^{3+} ratio in $Li_3Al_xY_{1-x}Cl_6$ (0<x<1). b) Schematic illustration of crystal representatives ccp type (cubic closed-packed anion sublattice) and hcp type (hexagonal-closed-packed anion sublattice) metal halide SSEs.

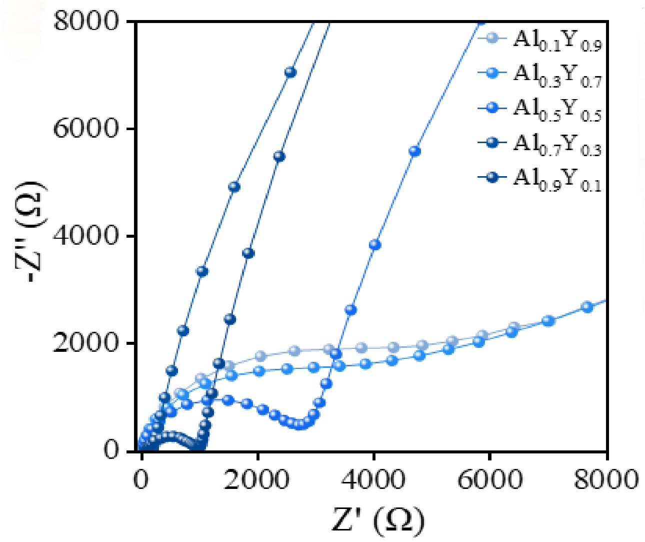

Figure S3. Impedance of LAYC with different Al^{3+}/Y^{3+} content at 25 °C.

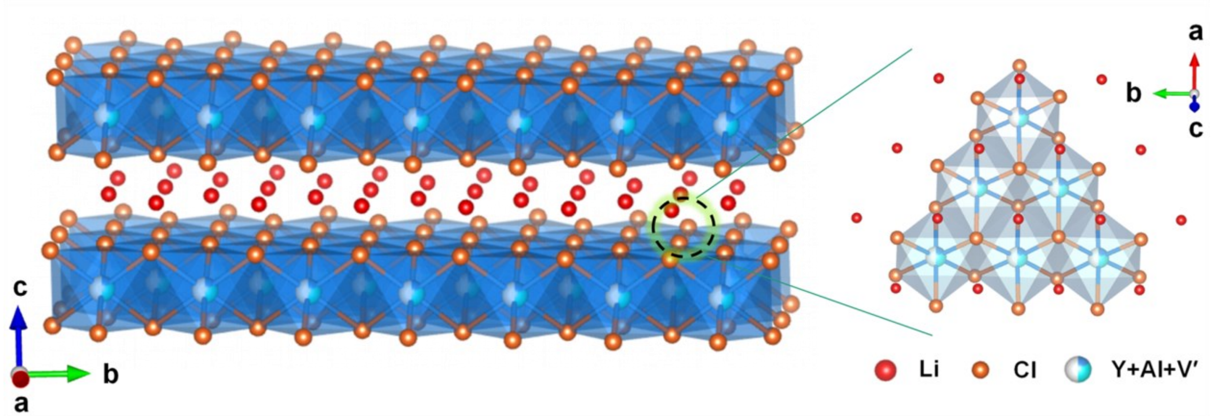

Figure S4. The structural model of LAYC.

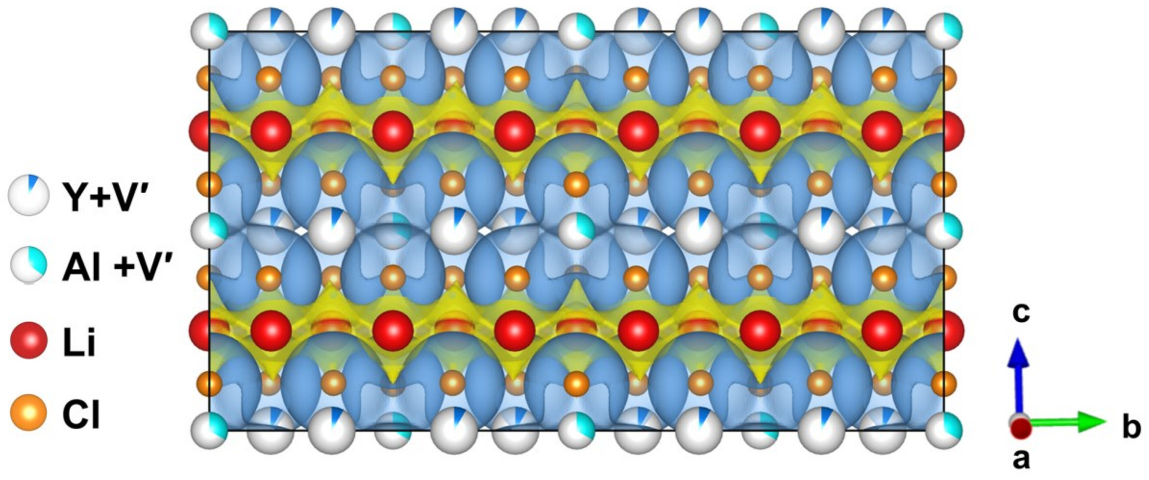

Figure S5. The structural model of LAYC with the Li-ion potential map.

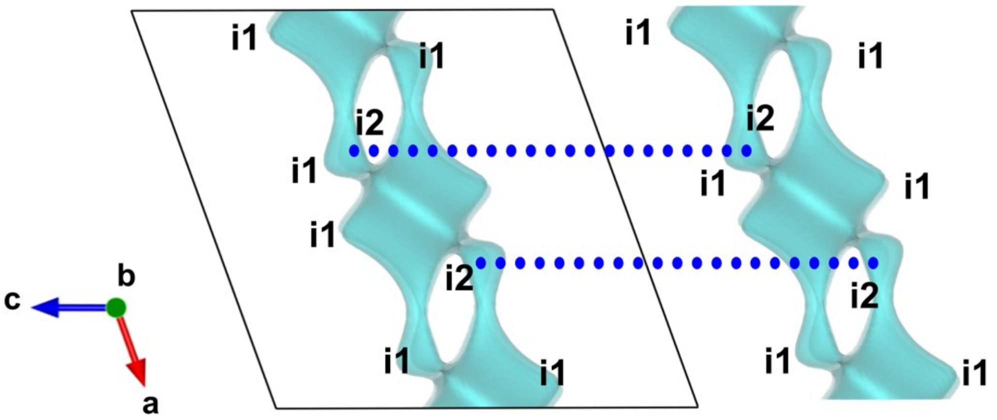

Figure S6. The migration pathway for lithium ions between the a-b planes in LAYC.

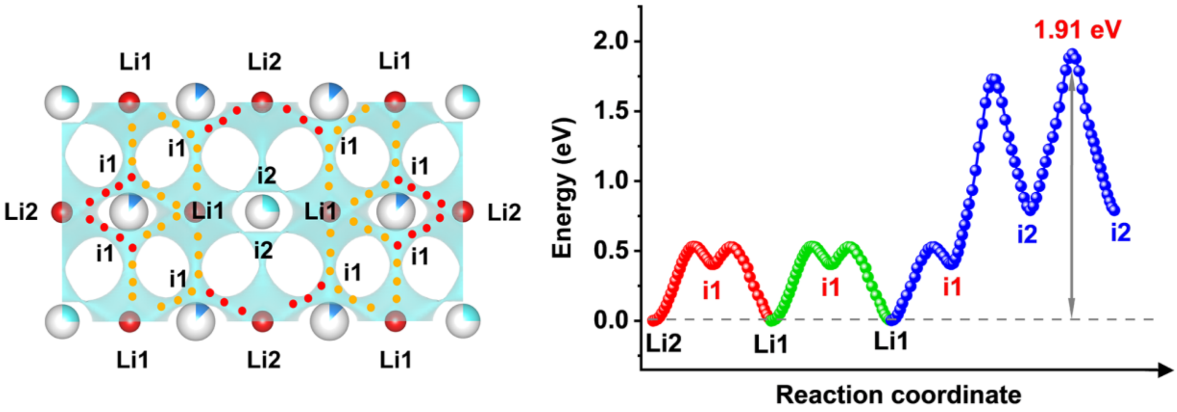

Figure S7. The migration pathway and migration barrier for lithium ions in $Li_3Al_{0.5}Y_{0.5}Cl_6$.

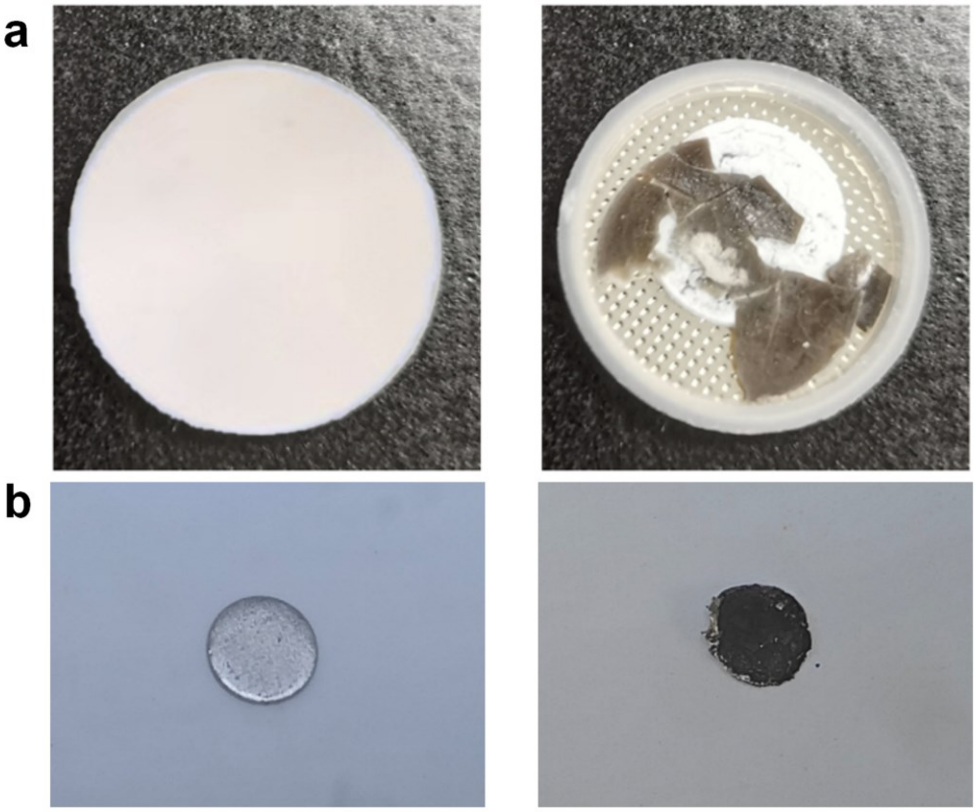

Figure S8. Morphology change diagram of lithium symmetrical battery before and after cycle. **(a)** LAYC. **(b)** Li metal.

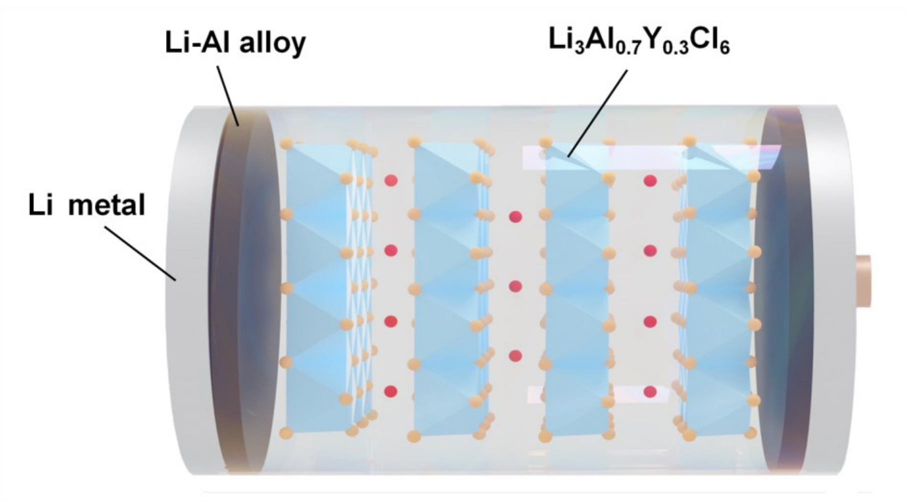

Figure S9. Schematic structure of Li|$Li_3Al_{0.7}Y_{0.3}Cl_6$|Li symmetric battery.

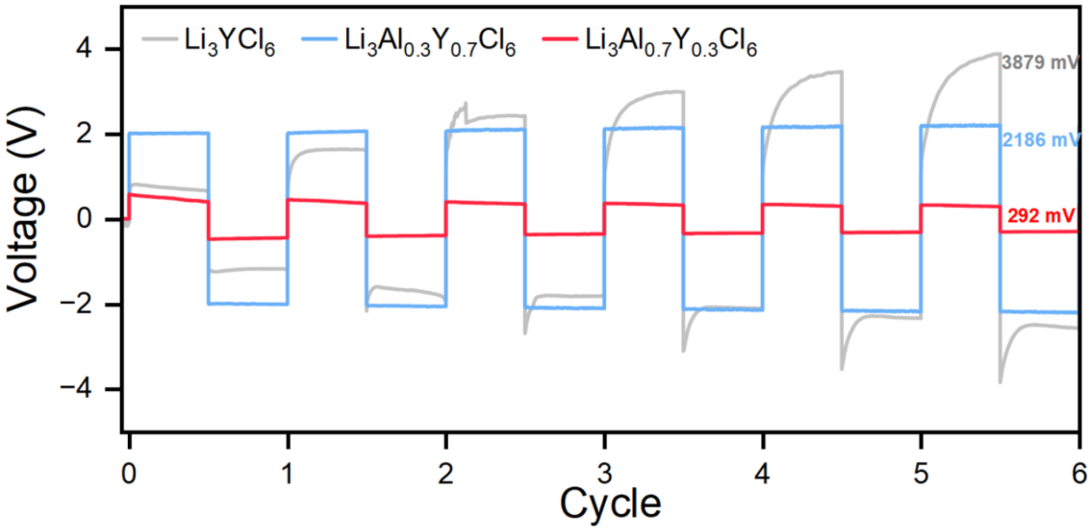

Figure S10. The constant current test of LYC and LAYC lithium symmetric batteries at 60 °C, 0.03 mA/cm^2.

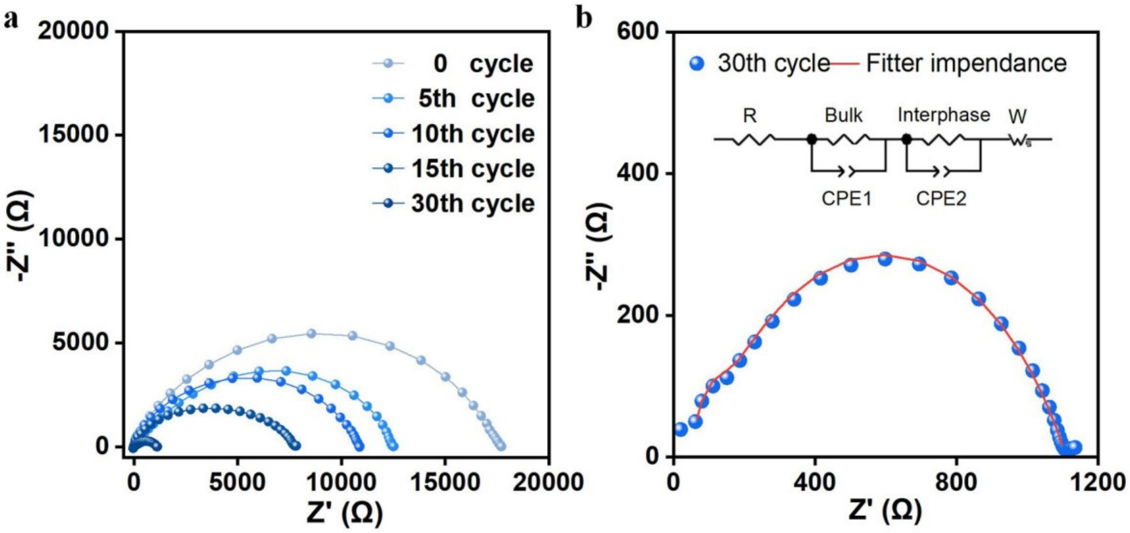

Figure S11. **(a)** The corresponding in-situ EIS testing in the first 30 cycles. **(b)** The 30th cycle impedance and fitting diagram of lithium symmetrical batter.

References

[1] Yin, Y. C. Yang, J. T. Luo, J. D. Lu, G. X. Huang, Z. Wang, J.P. Li, P. Li, F. Wu, Y. C. Tian, T. Meng, Y. F. Mo, H. S. Song, Y. H. Yang, J. N. Feng, L. Z. Ma, T. Wen, W. Gong, K. Wang, L. J. Ju, H. X. Xiao, Y. G. Li, Z. Y. Tao, X. Y. Yao, H. B. A $LaCl_3$-based lithium superionic conductor compatible with lithium metal. Nature. 2023, 616, 77-83.

[2] X. N. Li, J. T. Kim, J. Luo, C. T. Zhao, Y. Xu, T. Mei, R. Y. Li, J. W. Liang, X. L. Sun, Structural regulation of halide superionic conductors for all-solid-state lithium batteries. Nature Communications.. 2024, 15, 53.

[3] Adams, S.; Rao, R. P. Transport pathways for mobile ions in disordered solids from the analysis of energy-scaled bond-valence mismatch landscapes. Phys. Chem. Chem. Phys. 2009, 11, 3210−3216.

[4] Adams, S.; Prasada, R. R. Understanding Ionic Conduction and Energy Storage Materials with Bond-Valence-Based Methods. In Bond Valences. Struct. Bonding (Berlin); Brown, I. D.; Poeppelmeier, K.R., Eds.; Springer: Berlin/Heidelberg, 2014, 158, 129−159.

[5] Chen, H.; Adams, S. Bond softness sensitive bond-valence parameters for crystal structure plausibility tests. IUCrJ 2017, 4, 614−625.

[6] Chen, H.; Wong, L. L.; Adams, S. SoftBV−a software tool for screening the materials genome of inorganic fast ion conductors. Acta Crystallogr. Sect. B: Struct. Sci., Cryst. Eng. Mater. 2019, 75,18−33.

[7] Momma, K. Izumi, F. VESTA 3 for three-dimensional visualization of crystal, volumetric and morphology data. Journal of applied crystallography, 2011, 44, 1272-1276.